Available online at www.sciencedirect.com
ScienceDirect
Ceramics International 35 (2009) 2213–2218
CERAMICS INTERNATIONAL
www.elsevier.com/locate/ceramint

Electrochemical performance of LSM–SDC electrodes prepared with ion-impregnated LSM

Xingyan Xu [a], Chuanbao Cao [a,*], Changrong Xia [b], Dingkun Peng [b]

[a] *Research Center of Material Science, Beijing Institute of Technology, 100081 Beijing, China*
[b] *Laboratory for Renewable Clean Energy, Department of Materials Science and Engineering, University of Science and Technology of China, Hefei, 230026 Anhui, China*

Received 3 November 2008; received in revised form 29 November 2008; accepted 23 December 2008
Available online 22 January 2009

Abstract

$(La_{0.85}Sr_{0.15})_{0.9}MnO_{3-\delta}$ (LSM)–$Sm_{0.2}Ce_{0.8}O_{1.9}$ (SDC) (50:50 wt.%) composites, which are potential cathodes for intermediate-temperature solid oxide fuel cells, were prepared with a two-step fabricating process including screen-printing and ion-impregnation. SDC frame was screen-printed on electrolyte substrates and LSM was subsequently ion-impregnated to the SDC frame. The interfacial polarization resistances (area specific resistances) of the resulted electrodes were much lower than those prepared with a conventional screen-printing technique and also lower than those with impregnated SDC. At 700 °C, the total resistance was only 0.35 Ω cm^2 for an LSM–SDC electrode with impregnated LSM compared to 0.94 Ω cm^2 for a conventional electrode. Impedance spectroscopy was used to study the oxygen reduction kinetics within the electrodes. Three arcs were typically observed on the impedance spectrum. The high-frequency arc was attributed to oxygen ion transfer from the three-phase boundary to the electrolyte, while the intermediate-frequency arc was attributed to oxygen dissociation and adsorption. At high temperature, the arc due to gas phase diffusion was observed in the low frequency region, with size varying as $(Po_2)^{-0.76}$ and having low activation energy.

Keywords: LSM–SDC cathode; Ion-impregnation technique; Impedance spectroscopy; SOFCs; Solid oxide fuel cell

1. Introduction

$La_{1-x}Sr_xMnO_3$ perovskite (LSM) is regarded as one of the most promising cathode materials for solid oxide fuel cells (SOFCs) because of its high thermal and chemical stability [1]. It has shown promising performance for SOFCs operating at temperatures above 800 °C. However, due to its low ionic conductivity and high activation energy for oxygen disassociation, it is limited in the application of cathodes for intermediate-temperature SOFCs. To improve cathode performance, one strategy has been to replace LSM with higher catalytic activity at lower temperatures, particularly cobaltite-based cathodes. For example, $(La,Sr)(Co,Fe)O_3$-based cathodes have been optimized for the application in intermediate-temperature SOFC, especially with ceria-based electrolyte [2,3,4]. However, there are potential problems for mixed conductors including increased thermal expansion and higher apparent reactivity between electrode and electrolyte. An alternative strategy has been to combine a LSM with an ionic conducting second phase, such as ytrria-stabilized zirconia (YSZ) and doped ceria (DCO), in a composite matrix. This strategy has proven to be very promising to improve the electrochemical performance by extending the electrode–electrolyte interface. For example, Murray et al. [5,6] reported that, at 700 °C the interfacial resistance decrease from 7.82 Ω cm^2 for a LSM electrode to 2.49 Ω cm^2 for a LSM–YSZ (50:50 wt.%) composite, and further to 0.75 Ω cm^2 for a LSM–DCO (50:50 wt.%) composite. Xia et al. [7] prepared LSM–SDC composite cathode via a sol–gel process and found the polarization resistance of the composite cathode was only 0.28 Ω cm^2. Generally, the extent of the active interface extending for composite electrodes is very sensitive to the details of their microstructure, which is no doubts dependent on the fabrication processes. Often, the electronic conducting

* Corresponding author. Tel.: +86 10 68913792; fax: +86 10 68912001.
E-mail address: cbcao@bit.edu.cn (C. Cao).

0272-8842/$34.00
doi:10.1016/j.ceramint.2008.12.001

phase, LSM, and the ionic conducting phase are simultaneously coated onto the electrolyte substrate using a slurry-based process involving a mixed powder precursor, such as screen-printing. A more effective two-step process has been developed by Jiang et al. [8] to fabricate the composite cathode. In this process, nanosize GDC particles have been successfully introduced into the LSM cathode by ion-impregnation method and a pretty low cathode polarization resistance of 0.72 Ω cm^2 at 700 °C has been achieved. Recently, LSM–GDC (70:30 wt.%) composite powder was prepared through modification of LSM powder by $Gd_{0.2}Ce_{0.8}(NO_3)_x$ by Jiang et al. [9]. The electrode polarization of the LSM–GDC composite cathode at 700 °C under 500 mA/cm^2 was 0.42 Ω cm^2, which is close to that of pure LSM cathode at 850 °C under the same current density.

In our previous work, LSM–SDC composite electrodes were fabricated with the two-step fabricating process, where porous LSM frame was screen-printed onto dense electrolyte substrates and SDC was deposited into the frame using the ion-impregnation technique [10]. In this work, a different two-step process was developed for the fabrication of LSM–SDC electrodes. In this process, porous SDC frames were formed onto electrolyte substrates and LSM nanoparticles were then deposited into the SDC frame with the ion-impregnation process. The interfacial polarization resistances of the resulted LSM–SDC electrodes were compared with those prepared with the previous reported two-step process as well as the conventional screen-printing process. The highest electrode performance was observed for the electrode with impregnated LSM. In addition, oxygen transfer processes of the LSM–SDC electrode was also investigated using impedance spectroscopy.

2. Experimental

Electrolyte supports were prepared with $Sm_{0.2}Ce_{0.8}O_{1.9}$ (SDC) powder that was fabricated using an oxalate co-precipitation route with $Ce(NO_3)_3$ and Sm_2O_3 [11]. The resulted precipitate was pre-fired at 800 °C for 2 h to yield the SDC powder, which was then cold pressed into discs, sintered at 1350 °C for 5 h in air to form 1-mm-thick SDC pellets. The pellets were used as the electrolytes for cathodes. Electrode materials, $(La_{0.85}Sr_{0.15})_{0.9}MnO_3$ (LSM) and SDC, were prepared using glycine–nitrate method with nitrate salts [12]. The ash, produced through self-sustaining combustion of the nitrates and glycine, was heated in air at 800 °C for 2 h to remove possible carbon residue. SDC exhibited a fluorite structure and LSM a perovskite structure, which were confirmed with X-ray diffraction (X'pert PRO diffractometer with Cu Kα radiation) measurements.

Symmetrical LSM–SDC (50:50 wt.%) electrodes were fabricated onto SDC electrolytes using three routes. The first route concerns screen-printed SDC and impregnated LSM. SDC was ball-milled with the binder in acetone for 24 h to form uniform inks. SDC coating was applied to the electrolyte substrates by screen-printing, followed by sintering at 1000 °C for 2 h in air. SDC framework was therefore formed on the substrate. An aqueous solution containing 40.3 mol% La, 7.1 mol% Sr and 52.6 mol% Mn was prepared by dissolving the nitrate salts in distilled water. The solution was then deposited into SDC framework with an ion-impregnating technique, dried at room temperature and fired at 850 °C in air for 2 h. The mass of the electrode coating before and after the impregnation treatment was measured to estimate the impregnated oxide loading. The impregnation treatment was repeated to increase LSM loading until the weight of the impregnation matter is equivalent to that of the printed SDC. The derived electrode was named as LSM–SDC electrode with impregnated LSM. Microstructures and elemental mapping were revealed using JSM-6700F scanning electron microscopy. The second route consists of screen-printed LSM and impregnated SDC [10]. LSM was screen-printed onto the electrolyte substrates, while SDC was ion-impregnated into the porous LSM framework. The impregnation treatment was repeated until the weight of the impregnating SDC is equivalent to that of LSM. The resulted electrode was named as LSM–SDC electrode with impregnated SDC. And the third rout is the conventional electrode deposition technique. LSM–SDC composite was screen-printed onto the electrolyte substrates. The printed slurry was dried at about 200 °C under infrared lamp for 30 min and fired at 1000 °C for 2 h. The thickness All electrodes was approximately 40 μm with an effective area of 1 cm^2.

Interfacial polarization resistances were determined on symmetric cells with two-electrode configuration using AC impedance spectroscopy (ZAHNER IM6e). The frequency range was 0.01–10^5 Hz with signal amplitude of 5 mV. Measurements were conducted over a temperature range of 550–750 °C at oxygen partial pressures from 10^{-3} to 1 atm. We controlled the partial pressure of O_2 by mixing O_2 and N_2 gas streams. The flow rates of these gas flows were controlled by mass flow controlled and Po_2 was monitored by an oxygen sensor.

Thales software was used to fit the impedance data and to obtain equivalent circuits. In cases, one or two arcs overlapped, Thales was also used to determine the resistance values associated with each of the arcs.

3. Results and discussion

3.1. Effects of preparing procedure on interfacial polarization resistance

As shown in Fig. 1 LSM is most likely formed after the decomposition of impregnated lanthanum–strontium–manganese nitrate solution. Shown in Fig. 2 is the effect of preparing processes on area specific resistance (ASR) of LSM–SDC electrodes. ASR is typically used in the field of SOFC to quantify all resistances associated with the electrode, whether they occur at the gas/cathode interface, within the bulk of the cathode, or at the cathode/electrolyte interface [13]. The electrode prepared with the first route, impregnated LSM, has the lowest resistance while the one with the third route, conventional screen-printing, has the highest resistance. For example, at 700 °C the resistance decreases from 0.94 Ω cm^2 for screen-printed electrode to 0.48 Ω cm^2 for LSM–SDC

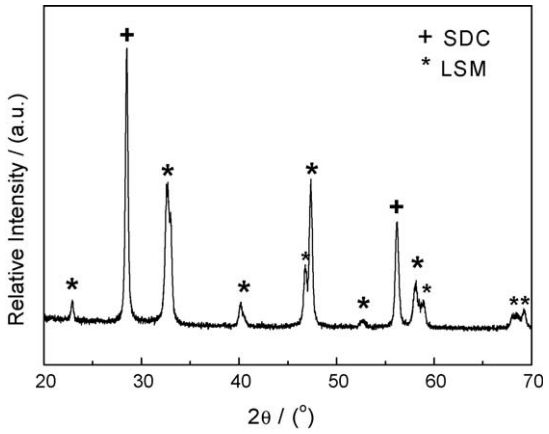

Fig. 1. XRD pattern for an LSM–SDC composite electrode with impregnated LSM.

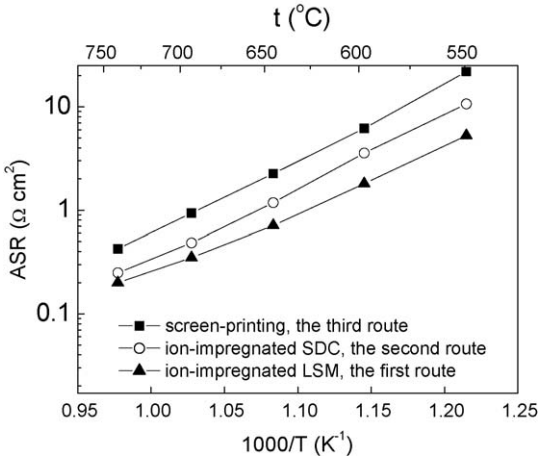

Fig. 2. Area specific resistance for LSM–SDC cathodes prepared with a screen-printing technique and two-step processes with ion-impregnated SDC and ion-impregnated LSM.

electrode with impregnated SDC, and further to 0.35 Ωcm^2 for the one with impregnated LSM. The reason is probably that electrodes prepared by ion-impregnating have small particles and increase TPBs, and then decrease the interfacial resistance [10]. While LSM–SDC electrode with impregnated LSM not only increases TPBs, but also improves catalytic performance due to large surface area of small LSM particle, resulting in promoted oxygen adsorption and dissociation rate, and therefore obtains the minimum resistance. The resistance of 0.35 Ω cm^2 for the one with impregnated LSM is about 2 times lower than that of LSM–GDC (50:50 wt.%) prepared by impregnated GDC [6], but slightly higher than that of LSM–GDC (50:50 wt.%) composite cathode via a sol–gel process [7]. Therefore, the extent of the active interface extending for composite electrodes is very sensitive to the details of their microstructure, which is no doubts dependent on the fabrication processes. Shown in Fig. 3a and b is SEM microviews for LSM–SDC electrodes prepared with the third and first route, respectively. Fig. 3a is a typical microstructure for porous composites electrode prepared by a conventional screen-printing technique. Before LSM impregnation, SDC frame had similar microstructure as shown in Fig. 3a. However, after impregnating process, the structure changed significantly. As shown in Fig. 3b, small LSM particles uniformly cover submicron SDC particles and increase TPBs. Shown in Fig. 4a is Mn, and Ce elemental dot maps, where LSM and SDC can be clearly identified. Shown in Fig. 4b is the corresponding line mapping. The content distribution curves are not smooth, but wave a lot. The waving is possibly due to the fact that the electrode is porous. However, the Mn mapping shows obviously that Mn was uniformly deposited inside porous SDC layer. Therefore, the high performance resulted from the ion-impregnation method is possibly due to effectively extending TPBs and large surface area of small LSM particle which promotes oxygen adsorption and dissociation rates.

3.2. Impedance spectroscopy of LSM–SDC electrodes with impregnated LSM

Shown in Fig. 5 is the impedance spectra for LSM–SDC electrodes with impregnated LSM. The impedance was measured at temperatures between 550 and 750 °C and oxygen partial pressure, Po_2, between 0.001 and 0.21 atm. The composition and microstructure etc. with relation to the oxygen reduction process can influence the measurement results. Besides, the measurement equipment can also influence the measurement results [14]. The conclusion is that although the standard resistor affects the measured impedance, the total

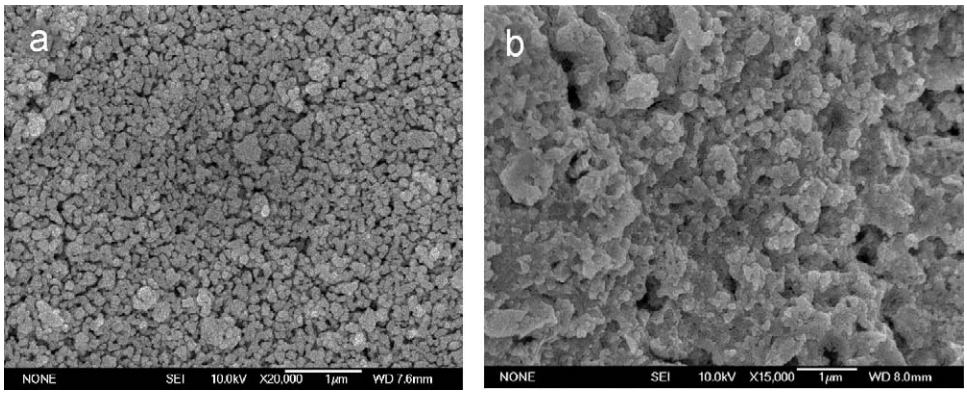

Fig. 3. SEM imagines of LSM–SDC cathodes prepared with (a) screen-printing technique and (b) process with ion-impregnated LSM.

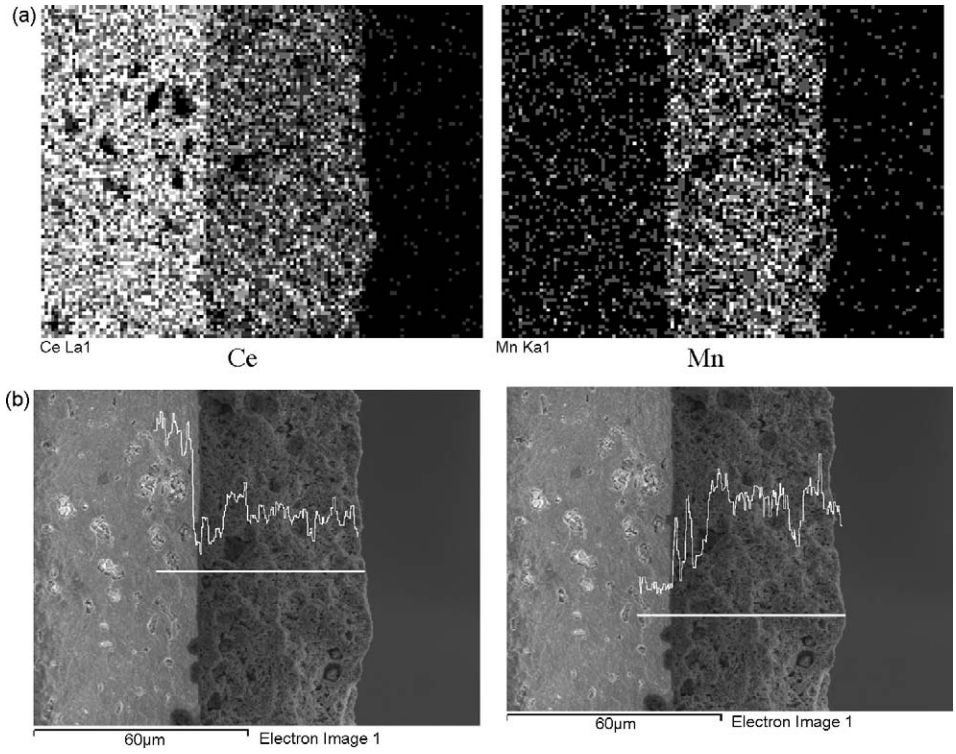

Fig. 4. Elemental dot mapping for an LSM–SDC electrode with impregnated LSM: (a) showing the elements Mn and Ce and (b) showing the variation in composition with distance from the SDC electrolyte.

polarization resistance may be determined with low error once the artifact has been recognized. Shown in Fig. 5, no poorly impedance spectroscopy can been observed; therefore, our experiment system has little effect on the measurement results. Complex impedance measurements typically produce two arcs at 550 °C, as shown in Fig. 5a. It indicates that two electrochemical processes control oxygen reduction at the cathode. With temperature increasing, high-frequency arc gradually disappears and an additional arc is present at low frequency, which indicates that the rate-limiting step changes. The impedance response at high frequency appears to be independent oxygen partial pressure, while those at intermediate frequency and low frequency show a significant dependence on the oxygen partial pressure.

These results were evaluated by using the equivalent circuit of Fig. 5d using Thales software. The first resistor, R_o, corresponds to the resistance of the electrolyte and the lead wires. (R_1Q_1), (R_2Q_2) and (R_3Q_3) represent the high-frequency arc, intermediate-frequency arc and low-frequency arc, respectively, where R is the resistance of the corresponding arc, and Q is a constant phase element representing time-dependent capacitive effects.

Fig. 6 shows the dependence of R on Po_2. The dependence of R_1 on Po_2 yields a slope n = −0.03. The weak Po_2 dependence of R_1 suggests that neither atomic oxygen nor molecular oxygen are involved in the step [15]. Therefore, the high-frequency arc could be interpreted as oxygen ion transfer from the TPB to the SDC electrolyte [5]. For composite electrodes, the electrochemical history can affect he measurement. A series of impedance measurements were performed; first at OCV, and then the electrode was polarized for certain time. After 200 mA/cm^2 current passing for 5, 30, 60 min, impedance was measured at OCV. Shown in Fig. 7 is the impedance responses measured at 600 °C, Po_2 = 0.21 atm, and different current passing time. It can be seen that with increasing time, the high-frequency arc remained nearly unchanged. This is understandable in that the oxygen vacancies created on the LSM surface do not affect oxygen ion transfer, which is a reaction between oxygen ions at the TPB and those in vacancies in the electrolyte.

R_2 varied as $(Po_2)^{-0.25}$ and the corresponding activation energy was 1.1 eV, abstracted from the slope of the linear plot of ln(1/R) vs. 1/T. The weak oxygen partial pressure dependence and high activation energy are similar to that of LSM–YSZ composites [16], which produced an activation energy of 1.49 and n = −0.29. This suggests the same rate-limiting mechanism, which is oxygen dissociation and adsorption. The effect of electrochemical history on the intermediate-frequency arc was shown in Fig. 7. There was no clearly change of the impedance responses for the LSM–SDC electrode with impregnated LSM. Such initial impedance behavior is quite different with that of conventional LSM–SDC and LSM–YSZ electrodes [17]. However, it is similar to those observed on $La_{0.6}Sr_{0.4}Co_{0.2}Fe_{0.8}O_3$ (LSCF) electrode [18]. This phenomenon indicates that LSM–SDC electrodes with impregnated LSM can provide abundant oxygen vacancies. Therefore, the oxygen vacancies appeared at LSM surface under cathodic polarization can be ignored.

As shown in Fig. 6, the Po_2 dependence of the low-frequency arc results in a slope n = −0.76, which illuminates that the low-frequency arc changes significantly with Po_2. The slope also

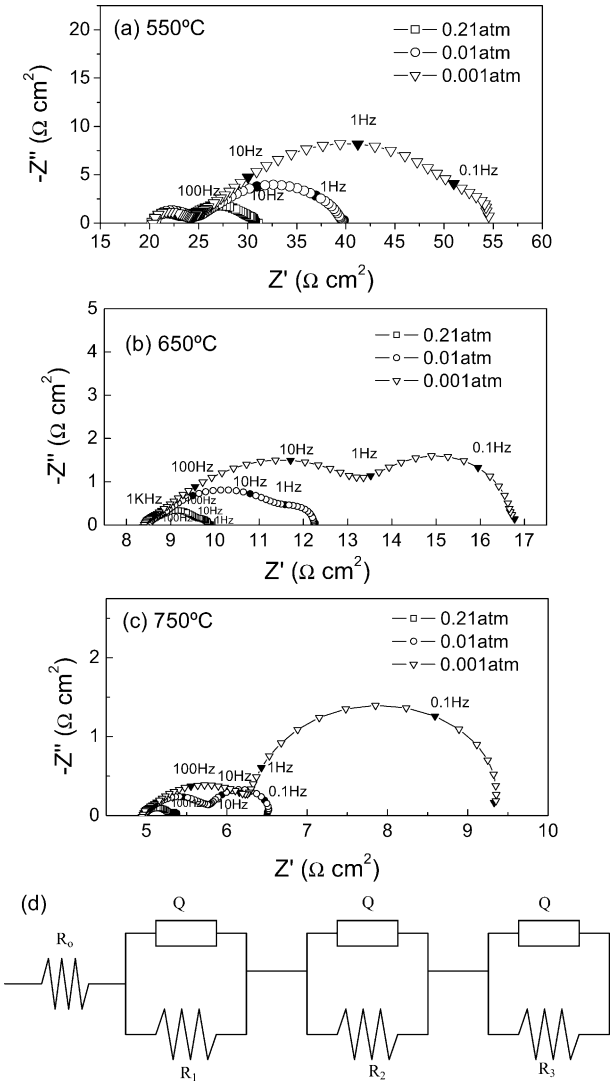

Fig. 5. AC impedance spectra measured at different oxygen partial pressure for an LSM–SDC electrode with impregnated LSM: (a) 550 °C, (b) 650 °C, (c) 750 °C, and (d) the model circuit.

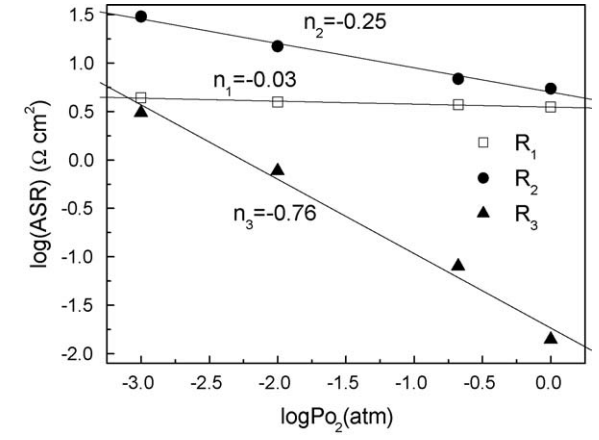

Fig. 6. Po_2 dependence for an LSM–SDC electrode with impregnated LSM.

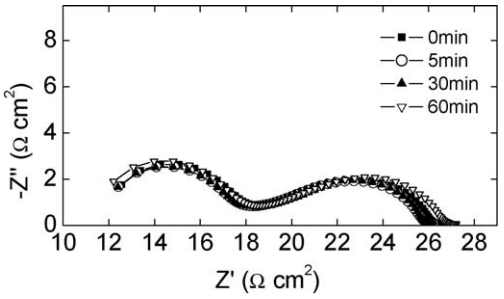

Fig. 7. Impedance responses measured at 600 °C, Po_2 = 0.21 atm and different 200 mA cm^{-2} passing time for an LSM–SDC electrode with impregnated LSM.

indicates that the low-frequency arc represents a complex step related to oxygen diffusion since n = −0.5 is usually considered to correspond to a surface diffusion step while n = −1.0 to a gas phase diffusion process [19,20]. Fig. 8 shows the impedance spectra measured at various temperatures (700 °C, 750 °C and 800 °C) and Po_2 = 0.001atm. It can be seen that the variation of the low-frequency arc is comparatively small in the range of measuring temperature. The activation energy of the low-frequency arc is therefore low. This reaction could be interpreted as the diffusion of oxygen molecules in electrode pores or surface diffusion. The activation energy of low-frequency arc is only 0.14 eV as calculated from the temperature dependence of R_3. If surface diffusion is the dominating step, the activation energy is usually about 2 eV, relatively higher than that of gas phase diffusion [21]. Therefore the low-frequency arc is attributed to gas phase diffusion, the activation energy of which is very low, and the gas phase diffusion flux resulting from the gradient in the chemical potential of the gas is proportional to the gas pressure.

The characteristics of LSM–SDC composite electrodes with impregnated SDC were also investigated by impedance spectroscopy [10]. Three arcs were observed in the impedance spectra. Oxygen ion transfer, charge transfer and surface diffusion of oxygen ions were found to be possible rate limiting steps for the high-frequency arc, intermediate-frequency arc, and low-frequency arc of the impedance spectra. While the LSM–GDC composite cathode prepared by slurry-coating was limited by oxygen ion transfer and oxygen adsorption for the high-frequency arc and low-frequency arc of the impedance spectra [6]. In this work, there is no unanimous agreement on the details of the oxygen reduction mechanism since the different microstructure of LSM-based composite electrodes prepared by three routes play an important role.

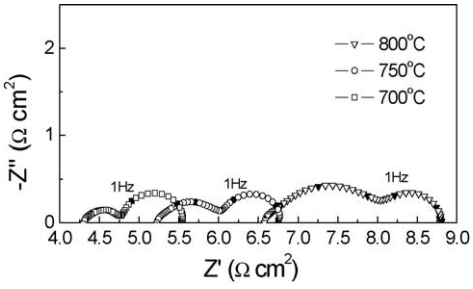

Fig. 8. AC impedance spectra measured at Po_2 = 0.001 atm for an LSM–SDC electrode with impregnated LSM.

4. Conclusion

LSM–SDC composite electrodes were fabricated using a two-step fabricating process with ion-impregnated LSM. The interfacial polarization resistance of this electrode is much lower than those of electrodes prepared with a conventional screen-printing technique or a process with ion-impregnated SDC. The characteristics of LSM–SDC electrodes were investigated by ac impedance spectroscopy. The high-frequency arc was attributed to oxygen ion transfer from the three-phase boundary to the electrolyte. The intermediate-frequency arc was attributed to oxygen adsorption and dissociation. The low-frequency arc was attributed to gas phase diffusion with a $(Po_2)^{-0.76}$dependence and low activation energy. Under applied cathodic potential, the interfacial resistance of LSM–SDC with impregnating LSM for the O_2 reduction were essentially independent of the cathodic current passage treatment, while the performance of cathode with impregnating SDC was affected by its electrochemical history, the interfacial polarization resistance decreases sharply at first and then slowly with time increasing.

Acknowledgements

The work was supported by the National Nature Science foundation of China (Nos. 50372066 and 50672096) and SRFDP 20050358023.

References

[1] N.Q. Minh, J. Am. Ceram. Soc., Ceram. Full Cells 76 (3) (1993) 563–588.
[2] E. Lust, G. Nurk, S. Kallip, I. Kivi, Electrochemical characteristics of $Ce_{0.8}Gd_{0.2}O_{1.9}|La_{0.6}Sr_{0.4}CoO_{3-\delta} + Ce_{0.8}Gd_{0.2}O_{1.9}$ half-cell, J. Solid State Electrochem. 9 (10) (2005) 674–683.
[3] B.C.H. Steele, J.M. Bae, Properties of $La_{0.6}Sr_{0.4}Co_{0.2}Fe0_{.8}O_{3-x}$ (LSCF) double layer cathodes on gadolinium-doped cerium oxide (CGO) electrolytes – II. Role of oxygen exchange and diffusion, Solid State Ionics 106 (3–4) (1998) 255–261.
[4] V. Dusastre, J.A. Kilner, Optimisation of composite cathodes for intermediate temperature SOFC applications, Solid State Ionics 126 (1–2) (1999) 163–174.
[5] E.P. Murray, T. Tsai, S.A. Barnett, Oxygen transfer processes in (La,Sr)MnO_3/Y_2O_3-stabilized ZrO_2 cathodes: an impedance spectroscopy study, Solid State Ionics 110 (3–4) (1998) 235–243.
[6] E.P. Murray, S.A. Barnett, (La,Sr)MnO_3–(Ce,Gd)O_{2-x} composite cathodes for solid oxide fuel cells, Solid State Ionics 143 (3–4) (2001) 265–273.
[7] C.R. Xia, Y. Zhang, M. Liu, LSM–GDC composite cathodes derived from a sol–gel process – effect of microstructure on interfacial polarization resistance, Electrochem. Solid State Lett. 6 (12) (2003) A290–A292.
[8] S.P. Jiang, Y.J. Leng, S.H. Chan, et al., Development of (La,Sr)MnO_3-based cathodes for intermediate temperature solid oxide fuel cells, Electrochem. Solid State Lett. 6 (4) (2003) A67–A70.
[9] Y.J. Leng, S.H. Chan, K.A. Khor, S.P. Jiang, $(La_{0.8}Sr_{0.2})_{(0.9)}MnO_3$–$Gd_{0.2}Ce_{0.8}O_{1.9}$ composite cathodes prepared from (Gd, Ce)$(NO_3)_{(x)}$-modified $(La_{0.8}Sr_{0.2})_{(0.9)}MnO_3$ for intermediate-temperature solid oxide fuel cells, J. Solid State Electrochem. 10 (6) (2006) 339–347.
[10] X.Y. Xu, Z.Y. Jiang, X. Fan, C.R. Xia, LSM–SDC electrodes fabricated with an ion-impregnating process for SOFCs with doped ceria electrolytes, Solid State Ionics 177 (19–25) (2006) 2113–2117.
[11] R.R. Peng, C.R. Xia, D.K. Peng, G.Y. Meng, Effect of powder preparation on $(CeO_2)_{(0.8)}(Sm_2O_3)_{(0.1)}$ thin film properties by screen-printing, Mater. Lett. 58 (5) (2004) 604–608.
[12] L.A. Chick, L.R. Pedersen, G.D. Maupin, J.L. Bates, L.E. Thomas, G.J. Exarhos, Glycine nitrate combustion synthesis of oxide ceramic powders, Mater. Lett. 10 (1–2) (1990) 6–12.
[13] Z.P. Shao, S.M. Haile, A high-performance cathode for the next generation of solid-oxide fuel cells, Nature 431 (7005) (2004) 170–173.
[14] M.J. Jorgensen, S. Primdahl, M. Mogensen, Characterisation of composite SOFC cathodes using electrochemical impedance spectroscopy, Electrochim. Acta 44 (24) (1999) 4195–4201.
[15] J. Hamagami, Y. Inda, T. Umegaki, K. Yamashita, High temperature pH sensing and O^{2-} conduction properties of electrophoretically fabricated ceria composites, Solid State Ionics 113–115 (1998) 235–239.
[16] J. Van Herle, A.J. McEvoy, K. Ravindranathan Thampi, A study on the $La_{1-x}Sr_xMnO_3$ oxygen cathode, Electrochim. Acta 41 (1996) 1447–1454.
[17] J.D. Kim, G.D. Kim, J.W. Moon, Y.I. Park, Characterization of LSM–YSZ composite electrode by ac impedance spectroscopy, Solid State Ionics 143 (3–4) (2001) 379–389.
[18] S.P. Jiang, A comparison of O_2 reduction reactions on porous (La,Sr)MnO_3 and (La,Sr)(Co,Fe)O_3 electrodes, Solid State Inoics 146 (1–2) (2002) 1–22.
[19] S.B. Adler, Mechanism and kinetics of oxygen reduction on porous $La_{1-x}Sr_xCoO_{3-\delta}$ electrodes, Solid State Ionics 111 (1–2) (1998) 125–134.
[20] E. Siebert, A. Hammouche, M. Kleitz, Impedance spectroscopy analysis of $La_{1-x}Sr_xMnO_3$-yttria-stabilized zirconia electrode kinetics, Electrochem. Acta 40 (11) (1995) 1741–1753.
[21] S.Z. Wang, Y. Jiang, Y.H. Zhang, et al., Promoting effect of YSZ on the electrochemical performance of YSZ + LSM composite electrodes, Solid State Ionics 113 (1998) 291–303.